14 Statistics of the ICRF2 Catalogue (CSJ)

This section will describe the ICRF2 catalogue. The catalogue is taken from a solution named gsf008a which produced angular positions for 3414 sources—more than five times the number of sources in the original ICRF1. However, 1966 sources were observed in only one session with the goal of densifying the catalogue. Hereafter in this section, we will refer to these sources as "survey" sources even though not all of them were observed in specially designed calibrator surveys such as the VLBA Calibrator Survey. The remaining sources which were observed in more than one session will be identified as "multi-session" sources.

14.1 Primary Distribution

Figure 42 shows the distribution over the sky of the 1448 sources which have been observed in at least two sessions. The color coding given in the figure's legend signifies the un-inflated 1-σ formal declination uncertainties.

14.2 Survey Distribution

Figure 43 shows the distribution over the sky of the 1966 single-session survey sources. The survey sources median un-inflated formal uncertainties are 406 and 571 μas, in $\alpha\cos(\delta)$ and δ respectively. The survey's median number of group delay observations is 41 and the median epoch of observation is 2004.4.

The rest of this section will focus on the remaining 1448 sources which were observed in at least two sessions. For these sources, we will look at the distribution of sources over the sky, the formal position errors, the number of observing sessions and group delays per source, and the distributions of mean, first and last epochs of observations as well as the total time span of observations per source. In all these ways we will characterize the ICRF2 observations.

14.3 Un-inflated formal uncertainties

Figure 44 shows the distribution of the un-inflated 1-σ formal uncertainties in Right Ascension arc-length for which the median is $\sigma_{\alpha\cos(\delta)} = 100$ μas. Figure 45 shows the distribution of the un-inflated 1-σ formal uncertainty in declination for which the median is $\sigma_\delta = 175$ μas. Both figures show $\log_{10}(\sigma)$ vs. $\log_{10}(N_{obs})$. A slope of -0.5 corresponds to the un-inflated formal uncertainties scaling as $1/\sqrt{N_{obs}}$ as one would expect from averaging white noise limited measurements. However, for small numbers of observations the observed slopes are steeper than -0.5 and become shallower as the numbers of observations increase. For sources with the largest numbers of observations the slope is nearly flat with a $\sigma \approx 10$ μas.

14.4 Number of observations

Figure 46 shows the distribution of the number of observing sessions per source for sources with a minimum of two sessions. The median number of sessions for these sources is 7. Note that over 400 sources have been observed in only a few sessions.

Figure 47 shows the distribution of the number of group delay measurements per source plotted on a log scale. The median number of delay observations per multi-session source is 156. Note the strong peak near 100 observations.

Some sources that have long been used for geodetic and earth orientation sessions have more than 10,000 observations and a few even have more than 100,000 observations. The unevenness in the distributions of both sessions and delay observations results from the ICRF2 database being built in large part from programs whose primary goals were not building a celestial frame, but rather measuring plate tectonics or earth orientation. Programs to densify the ICRF1 have been very successful as was seen in Figs. 42 and 43, but the densification programs typically are resource limited to observe each source in only a few sessions.

14.5 Observing Epochs

Figure 48 shows the distribution of the mean epoch of observation for the 1448 multi-session sources. The median mean epoch is 2001 with the vast majority of the source mean epochs being between 1994 and 2007. Figure 49 shows the distribution of the first epoch of observation for the 1448 multi-session sources. The median first epoch is 1995.5. Figure 50 shows the distribution of the last epoch of observation for the 1448 multi-session sources. The median last epoch is 2008. About half of the 1448 sources have been observed within the last few years and the vast majority of the sources have been observed since 1995—the data cutoff date for the original ICRF1.

Finally, Figure 51 shows the distribution of observing span in years for the 1448 multi-session sources. As just explained, the distribution of observations is very uneven. From this figure we note that about 250 sources have spans of about a year or less. At the other extreme, there are a few sources that were used in early geodetic and earth orientation programs that have 23–30 year spans. After the mid-1980s the Mark III observing system increased sensitivity resulting in more sources being observed. We see this reflected the increase in the distribution height for sources with spans less than 23 years.

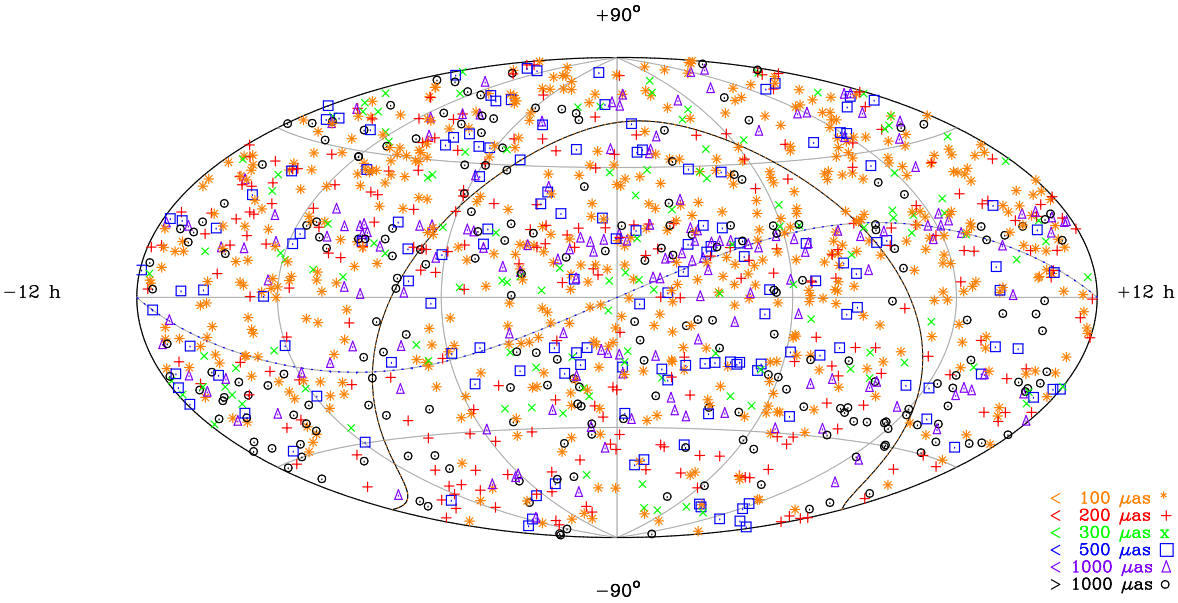

Figure 42: gsf008a distribution of 1448 multi-session sources (at least 2 observing sessions). The un-inflated 1-σ formal declination errors are color coded according to the legend in the figure. The median $\sigma_\delta = 175$ μas. The center is $(\alpha, \delta) = (0, 0)$. The Galactic plane is the roughly Ω-shaped line surrounding the center. The ecliptic plane is the dashed line. The single-session survey sources used to densify are shown in the next figure, Figure 43.

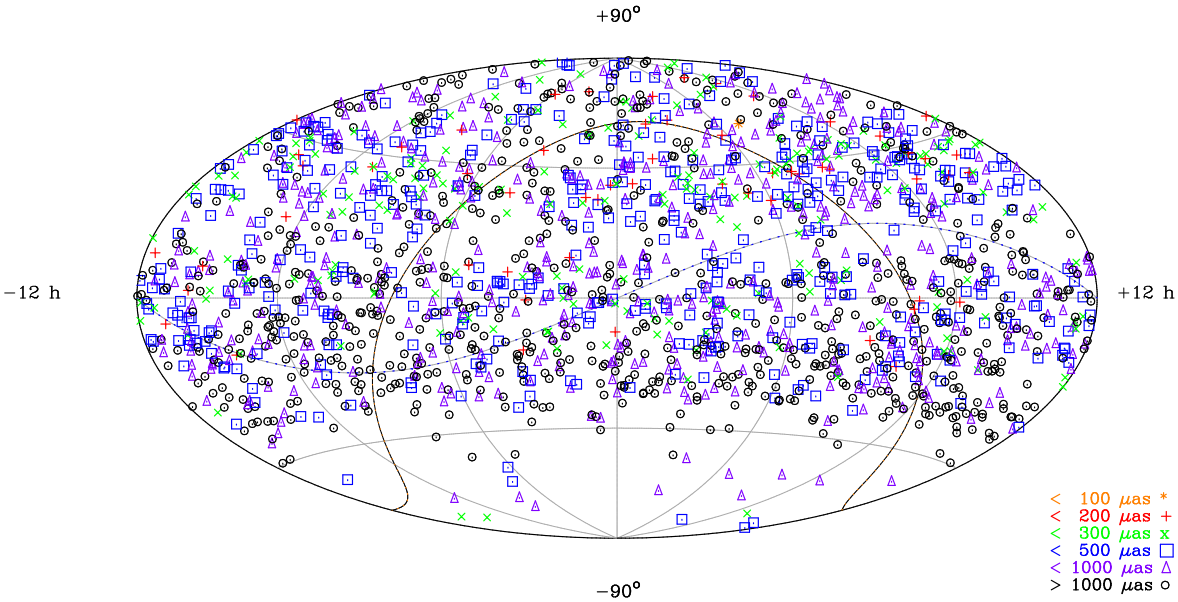

Figure 43: gsf008a survey distribution of 1966 single-session sources. The un-inflated 1-σ formal declination errors are color coded according to the legend in the figure. The median $\sigma_\delta = 751$ μas. The center is $(\alpha,\delta)=(0,0)$. The Galactic plane is the roughly Ω-shaped line surrounding the center. The ecliptic plane is the dashed line.

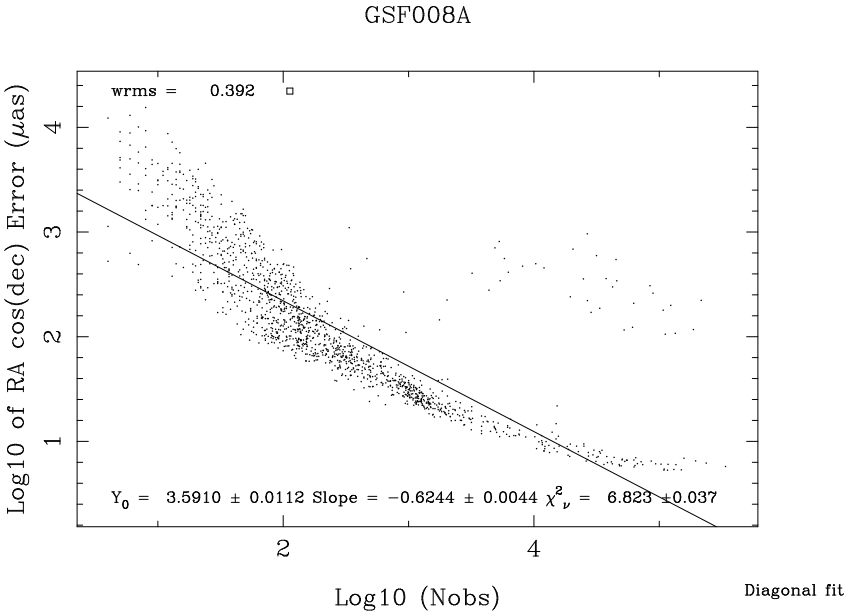

Figure 44: gsf008a catalogue's dependence of un-inflated $\sigma_{\alpha\cos(\delta)}$ on the number of observations for sources observed in at least two sessions. A slope of -0.5 would correspond to $1/\sqrt{N_{obs}}$ averaging of white noise. Calibrator survey's ≈ 2000 single-session densifying sources are not shown.

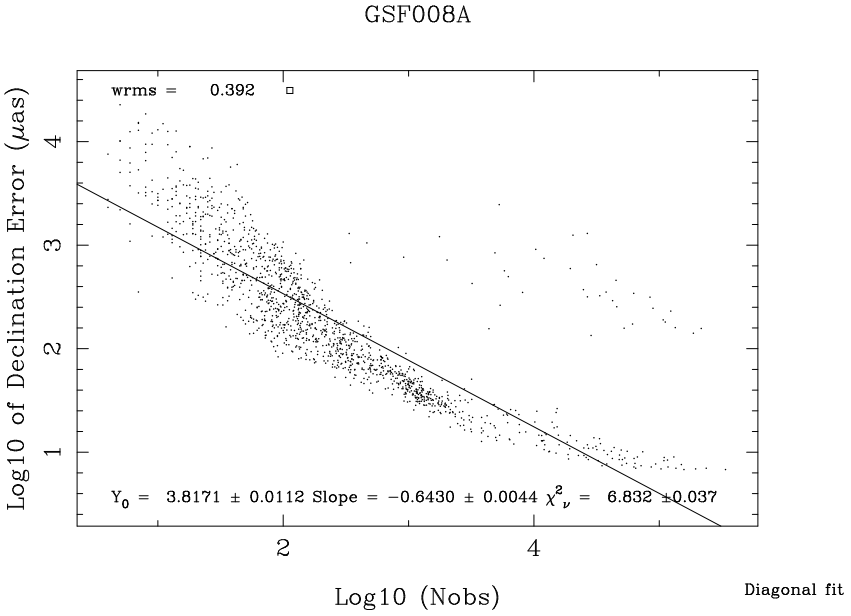

Figure 45: gsf008a catalogue's dependence of un-inflated σ_{δ} on the number of observations for sources observed in at least two sessions. A slope of -0.5 would correspond to $1/\sqrt{N_{obs}}$ averaging of white noise. Calibrator survey's ≈ 2000 single-session densifying sources are not shown.

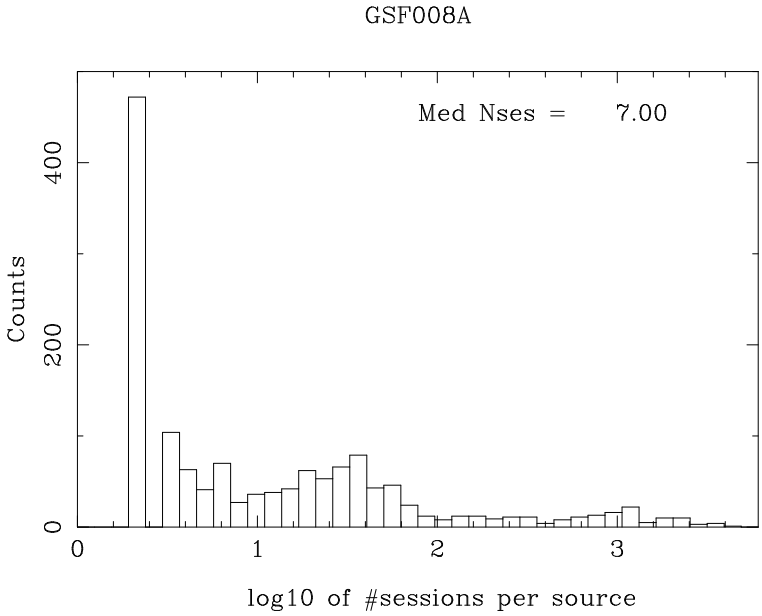

Figure 46: gsf008a catalogue's distribution of the number of observing sessions per source for sources with at least two sessions. The median number of sessions per source is 7 excluding the set of ≈ 2000 single-session densifying sources (not shown) from calibrator surveys.

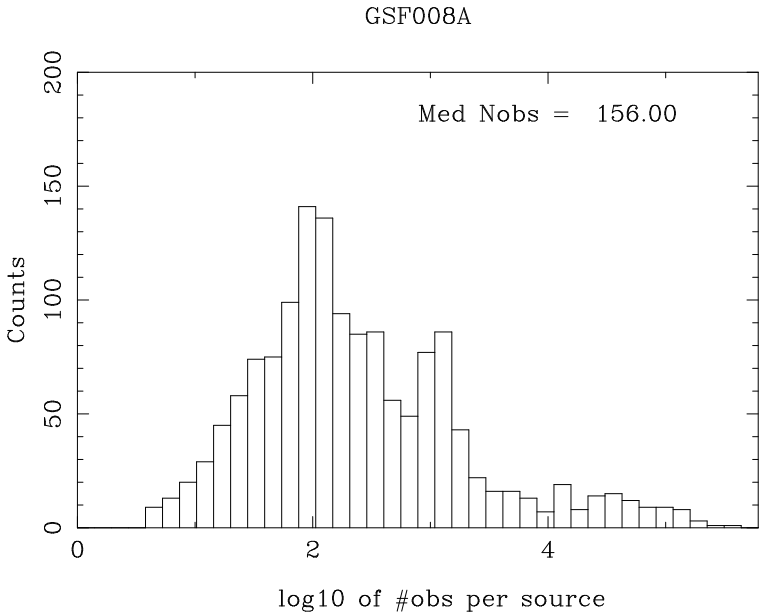

Figure 47: gsf008a catalogue's distribution of the number of group delay measurements plotted on a log scale for sources observed in at least two sessions. Note the strong peak near 100 observations. Calibrator survey's ≈ 2000 single-session densifying sources are not shown.

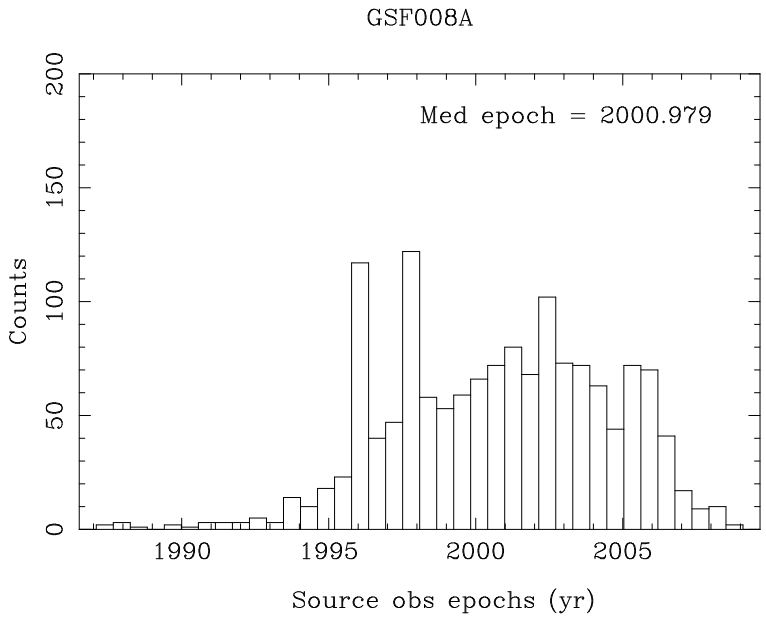

Figure 48: gsf008a catalogue's distribution of mean observing epoch for sources observed in at least two sessions. Calibrator survey's ≈ 2000 single-session densifying sources are not shown.

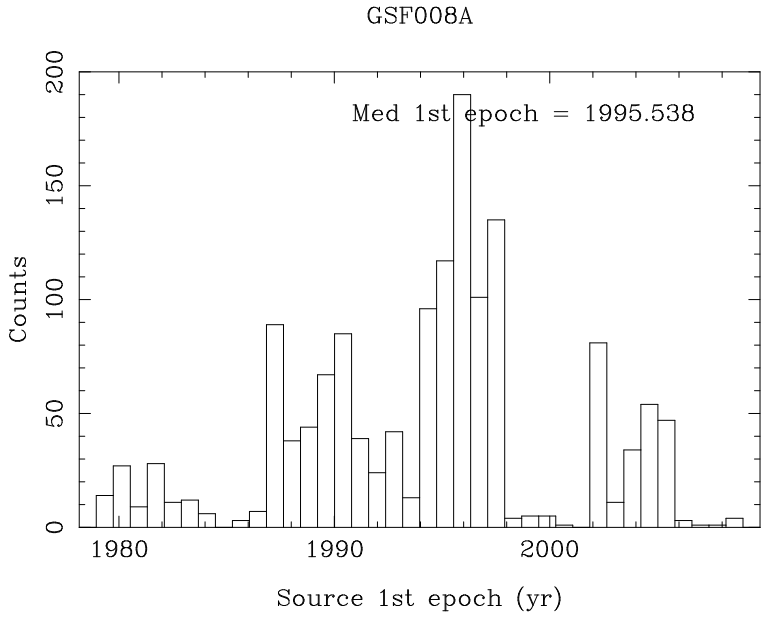

Figure 49: gsf008a catalogue's distribution of first observing epoch for sources observed in at least two sessions. Calibrator survey's ≈ 2000 single-session densifying sources are not shown.

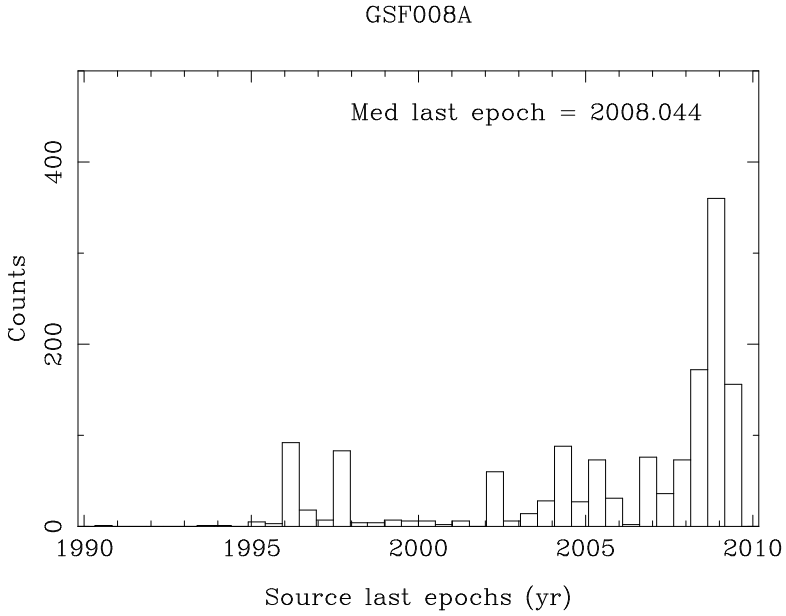

Figure 50: gsf008a catalogue's distribution of last observing epoch for sources observed in at least two sessions. Calibrator survey's ≈ 2000 single-session densifying sources are not shown.

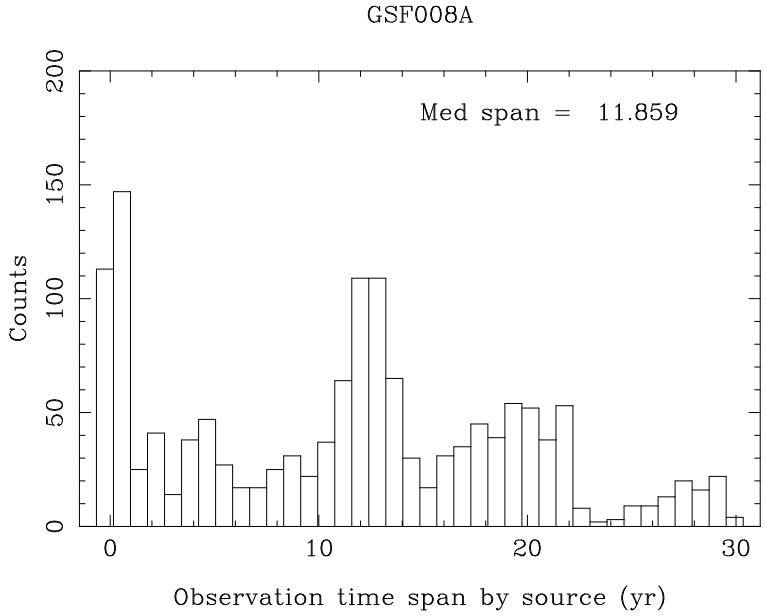

Figure 51: gsf008a catalogue's distribution of observing span for each source which was observed in at least two sessions. The observation spans are very unevenly distributed from zero to 30 years with a median of about 12 years Calibrator survey's ≈ 2000 single-session densifying sources are not shown.